Digital Object Identifier 10.1109/TSG.2018.2888687

IEEE Transactions on Smart Grid, Early Access, 2018.

Real-Time Primary Frequency Regulation using Load Power Control by Smart Transformers

Giovanni De Carne
Giampaolo Buticchi
Marco Liserre
Costas Vournas

Suggested Citation

G. De Carne, G. Buticchi, M. Liserre and C. Vournas, "Real-Time Primary Frequency Regulation using Load Power Control by Smart Transformers," in IEEE Transactions on Smart Grid, Early Access.

Real-Time Primary Frequency Regulation using Load Power Control by Smart Transformers

Giovanni De Carne, *Member, IEEE,* Giampaolo Buticchi, *Senior Member, IEEE,* Marco Liserre, *Fellow, IEEE,* and Costas Vournas, *Fellow, IEEE*

***Abstract*—In the last years the energy production share of power electronics-based generators has kept increasing with respect to the synchronous generation. These power electronics-resources do not offer rotational inertia, resulting in a decrease of the total system inertia and thus in larger frequency deviations during disturbances. Among several corrective solutions studied in literature, controlling the load consumption is a promising one. Fast in power response and widely distributed in the grid, load control is able to work as power reserve (both upwards and downwards) during frequency variations. In this regard, a Smart Transformer (ST) based solution is proposed. The ST is able to shape load consumption accurately by means of an On-Line Load sensitivity Identification-based (OLLI) control, and can support the primary frequency regulation in the power system. This paper presents an ST-based Real Time Frequency Regulation (RTFR) controller that varies load consumption by means of a voltage-based load control, in response to the frequency deviation in the power grid. The proposed method is described analytically and tested by means of a Power-Hardware-In-Loop experiments, in order to show the effectiveness of the RTFR controller in real time conditions and applications.**

***Index Terms*—Smart Transformer, Solid State Transformer, load sensitivity identification, frequency regulation, load control, demand response.**

I. Introduction

The increasing integration of Distributed Generation (DG), due to the converter-based connection, reduces the inertia of the grid, increasing frequency deviation following disturbances. A reduced grid inertia can affect the grid stability in the most severe cases [1] [2]. With this assumption, an unexpected event (e.g., fault, generator disconnection, or line tripping) challenges the stability of the system. A violation of the power quality standard (under- or over-voltage/frequency violations) can occur, and, in extreme cases, it may trigger a cascade of failures that leads to regional or national blackouts. Control actions for supporting the frequency are based on firm under-frequency load shedding [3], inertia control and frequency droop characteristic of wind turbines [4] [5], and energy reserves, for instance Battery Energy Storage Systems (BESS) [6] [7] or HVDC [8].

Another possibility is to interact directly with the loads to impact on the power system behavior. The advantages in controlling the load consumption lie on the distributed availability of control points in the grid and the fast dynamics in responding to operator requests [9]. For example, the demand response strategy enables the use of the demand consumption as spinning reserve in the case of active power deficiency [10] or to provide primary frequency regulation support [11]–[13]. However, several issues are expected in this direction, due to the need of a large communication infrastructure and privacy concerns on the data requested by smart meters, that may limit the application of demand response [14]. As an alternative, the load consumption can be modulated by controlling the grid voltage [15], [16] or using the concept of Electric Spring (ES) [17]–[20]. Exploiting voltage-sensitive loads, the voltage can be varied to adapt the load consumption to the desired level. This gives the possibility to manage load consumption in a practical and manageable manner, without involving complex and extensive communication infrastructure. As noted in [16], load power controllability in the order of 2 GW can be achieved in UK. In addition to the academia proposal, ENTSO-E has shown interest in letting the loads participate to services provision [21], whereas in countries like France, Spain, Belgium and Poland, loads can participate actively to balancing services.

An overview of the power system is shown graphically in Fig. 1, where several agents are involved in frequency regulation: conventional synchronous generators vary their power output ΔG_i through governors action and energy storage systems or High Voltage DC (HVDC) systems can respond to frequency variations by adapting their power output ΔE_i.

In the case of the HVDC systems, a Frequency Limit Control [8], [22] can be implemented, exploiting the fast ramp characteristics offered by the power electronics. In the case of frequency variation, the HVDC can provide an excess or a reduction of power in order to compensate for the frequency oscillation. Although an effective solution, given the availability of a considerable power reserve, to reduce the impact on the power systems, rate limiters are used to shape the power variation profile.

As highlighted in Fig. 1, this paper proposes a "Real Time Frequency Regulation" (RTFR) controller, realized by Smart Transformers (STs), power electronics transformer that interface the MV and LV grids. Given the control capability of these power converters, when the system frequency f

The research leading to these results has received funding from the European Research Council under the European Union's Seventh Framework Programme (FP/2007-2013) / ERC Grant Agreement n. [616344] - HEART, and from the German Federal Ministry of Education and Research (BMBF) within the Kopernikus Project ENSURE "New ENergy grid StructURes for the German Energiewende" (03SFK1I0).

Giovanni De Carne and Marco Liserre are with the Chair of Power Electronics, University of Kiel, Germany, e-mail: gdc@tf.uni-kiel.de

Giampaolo Buticchi is with the University of Nottingham Ningbo, China (UNNC), e-mail: buticchi@ieee.org

Costas Vournas is with the School of Electrical and Computer Engineering, National Technical University of Athens, Greece email: vournas@power.ece.ntua.gr

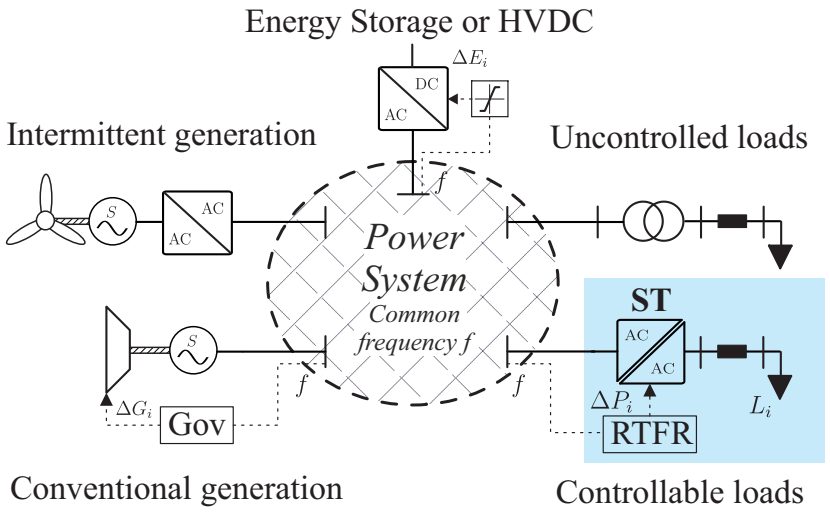

Fig. 1. Frequency regulation actors in the power system: the ST-fed grid is asynchronously-connected with the power system (blue square).

varies, the voltage-dependent load power consumption ΔP_i is modified accordingly, by controlling the voltage in the ST-fed grid within the allowed limits. Reactive power of the MV grid is unaffected because of the power electronics.

The paper is structured as follows: section II describes the Smart Transformer concept and the Real Time Frequency Regulation controller is explained; the contribution of the RTFR controller to the frequency regulation in the power grid is shown in section III; the validity of the approach is tested by means of a Power-Hardware-In-Loop setup described in section IV, and the results shown in section V. Section VI draws the conclusion.

II. ST-based Real Time Frequency Regulation control

The Smart Transformer is a power-electronic based transformer [23] [24], which can shape the load consumption of voltage-sensitive loads controlling the output voltage waveform [25]. An on-line estimation of the active power load sensitivity to voltage (as in [26]) allows for a high control accuracy of voltage-based control actions.

A. Concept and Control

In Fig.2 two alternative ST asynchronously-connection solution are shown: (a) the solid state transformer (SST) (Fig.2a), with the isolation in the DC/DC stage, and (b) the back-to-back solution (Fig.2b), where the isolation is guaranteed by an external conventional transformer. Both configurations allow for the independent control of the distribution grid. It may be argued that the initial investment for STs can be higher than other proposed methods. However, business cases developed within LV-ENGINE project have demonstrated that the ST can bring cost savings up to $£60m$ by 2030 and more than $£500m$ by 2050 at national level in UK [27], and reduce grid infrastructure reinforcements, like larger cables or higher ratings transformers.

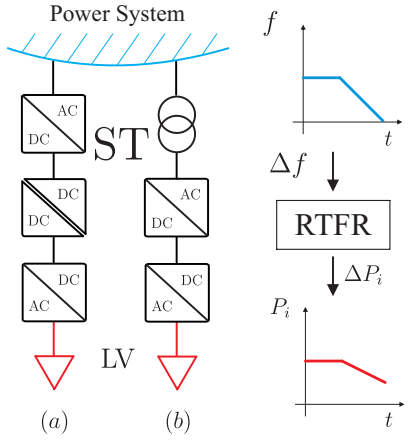

Fig. 2. Frequency regulation by means of (a) Solid State Transformer-based ST, and (b) back-to-back ST solution.

The RTFR controller shown in Fig. 2 can help regulate large frequency variations in the power system and thus avoid the activation of load shedding schemes.

To achieve the desired power change, the active power load sensitivity to voltage has to be calculated in advance. It has already been demonstrated in [26], that, the ST, by means of the OLLI algorithm, is able to estimate load sensitivity in real time and to update it within a certain time interval. The sensitivity measurement only lasts few seconds so it can be repeated every few minutes or more often, if deemed necessary. The basic idea of the OLLI is to apply a ramp variation of the chosen variable (e.g., voltage) and to measure the active and reactive power consumption during the ramp, allowing the voltage and frequency load sensitivity coefficients computation. In this paper, only the voltage dependence of load active power is considered. The ST-fed grid is asynchronously connected to the main power system. Whereas the active power consumption has an impact on main grid frequency, the load reactive power is provided by the LV converter without affecting on the main power system. The

concept to vary the voltage to control a certain load has been also explored with the Electric Spring concept [17], [18], where the voltage across a non-critical load is controlled to shape the power consumption for providing services to the grid (e.g., voltage regulation). However, the Smart Transformer does not require active/reactive support to control load power, while it can also control reactive power injection in the MV grid. Also, the Electric Spring has to be implemented in each load, and thus it requires to be spread in the distribution grid, whereas, the Smart Transformer replaces the conventional transformer, and thus has higher control.

B. Control Implementation

At specified time instants during the voltage variation the line currents and phase-to-ground voltages are measured, and the single-phase active and reactive powers P and Q and rms voltage V are calculated. Using the measured values at time t_k and the previous time instant t_{k-1}, the active power sensitivity to voltage K_p and K_q at time t_k are computed as in [26]:

$$K_p = \frac{\frac{P(t_k)-P(t_{k-1})}{P(t_{k-1})}}{\frac{V(t_k)-V(t_{k-1})}{V(t_{k-1})}} \tag{1}$$

This sequence is repeated in the following time instant until the end of the voltage ramp. The final value of the sensitivities is obtained averaging all the values stored during the time window considered.

Once the active power sensitivity to voltage is calculated for all three phases, the balanced voltage V to be applied to obtain the desired power variation ΔP is derived, as described in [25]:

$$V = \frac{\Delta P + (P_A K_{pA} + P_B K_{pB} + P_C K_{pC})}{\frac{P_A}{V_A} K_{pA} + \frac{P_B}{V_B} K_{pB} + \frac{P_C}{V_C} K_{pC}} \tag{2}$$

where K_{pA}, K_{pB}, and K_{pC} are the active power sensitivity to voltage in phase A, B, and C respectively. Assuming the initial three phase voltages with equal amplitude simplifies (2) using V_A=V_B=V_C=V_0:

$$\frac{V}{V_0} = 1 + \frac{\Delta P}{P_A K_{pA} + P_B K_{pB} + P_C K_{pC}} \tag{3}$$

Thus the p.u. voltage variation to be applied for achieving a certain power variation ΔP is obtained. The voltage set-point, however, must be constrained within the minimum and the maximum voltage limit.

The power set-point ΔP is calculated by measuring system frequency in the MV side of the ST. As shown in Fig. 3, if a variation of frequency is measured, the controller sets the power modulation ΔP^* following the droop characteristic shown in Fig. 4. A dead-band (e.g. $d = \pm 200\,\text{mHz}$) is assumed, in order to avoid the ST intervention in case of small frequency variations, caused by temporary load/generation unbalances. This value has been chosen in order to have a dead-band 10 times bigger than the one implemented in the generators governor: in [28] it is stated that the generator dead-band may vary from $0.02\,\%$ to $0.06\,\%$ of the nominal speed, that corresponds to $10\,\text{mHz}$ to $30\,\text{mHz}$ for a $50\,\text{Hz}$ system,

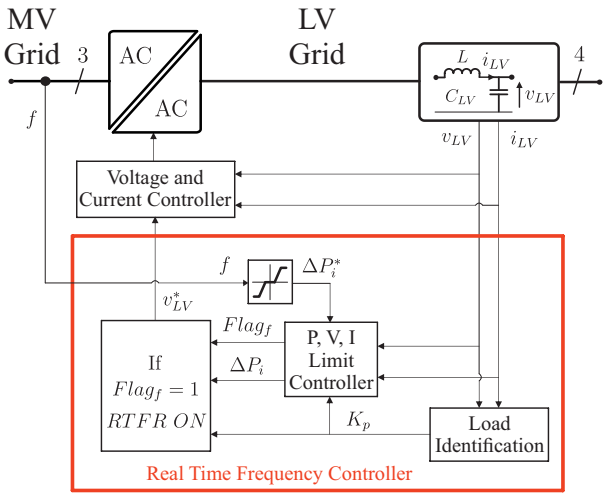

Fig. 3. On-Line Load sensitivity Identification and Control scheme

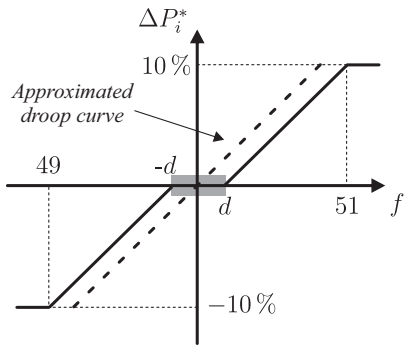

Fig. 4. Frequency/power characteristic implemented in the RTFR controller (continue line), and approximated droop curve used for analytical studies.

respectively. Lower case letters in Fig. 3 (e.g. v, i) refer to instantaneous values $v(t)$, $i(t)$.

Since the proposed system implies a closed-loop control, the damping effect could be achieved even without a precise system identification. However, with the OLLI algorithm, the power can be precisely controlled, offering superior service quality and guaranteeing to the customers that the curtailment is within the terms of agreement. The power modulation request ΔP^* is limited, as seen in Fig. 4, in order to maintain the power quality in the ST-fed LV grids. If the ST measures a frequency deviation, it applies the voltage variation to shape the load consumption, applying relation (3). In order to limit the power quality impact on the LV grid, the ST restores the voltage nominal value after the frequency transient ends and the frequency value is inside the controller dead-zone. The RTFR goal is to support synchronous generators during primary frequency control, increasing system damping, decreasing transient frequency deviations, and not to provide secondary frequency regulation. Since the secondary frequency regulation lasts for tens of minutes, the ST-fed loads could be affected by large voltage deviations (e.g., $\pm 5\%$) for several minutes, decreasing the quality of the service for a too long time window.

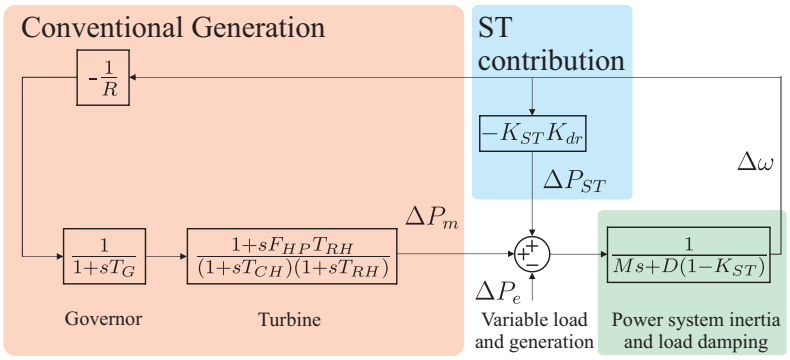

Fig. 5. Equivalent power system model with ST RTFR controller (in blue).

C. Voltage dependent loads in distribution grids

Since the RTFR approach exploits the load dependence on voltage, it is of concern to discuss the availability of such loads in distribution grid. In recent years, the control of electric appliances goes more in the constant power load direction, due to the converter interface with the grid. However, a large amount of voltage dependent loads are still present in the distribution grid. As highlighted in [29], these loads, such as air conditioner, induction lights, microwaves, and refrigerators, have a consistent constant impedance contribution in the power absorption. If these loads are considered in a residential grid together with other constant power loads, the aggregate load is still sensitive to voltage variation, even if in less-than-linear way (i.e., $K_p < 1$ pu) [29]. Field experiments have been carried out to determine the aggregate load sensitivity to voltage. In [30], the Serbian distribution grid showed voltage sensitivity K_p varying from 1.1 pu to 1.4 pu, that indicates a more-than-linear power change following a voltage variation. In a more recent publication [16], field trials have shown that the UK distribution network behaves as constant current load (i.e., $K_p \approx 1$ pu), guaranteeing reasonable power margin for voltage-based control actions.

Thus the RTFR control by means of Smart Transformer is a viable solution to provide primary frequency regulation.

III. System Frequency Regulation Analysis

In order to assess the effectiveness of the RTFR controller to regulate the transmission grid frequency, the frequency regulation loop shown in Fig. 5 is considered.

The analyzed system consists of an equivalent governor - turbine (reheat steam system), the rotating machines inertia and load self-regulation. The governor control is represented with a frequency/power droop characteristic $-1/R$. The governor dynamic behavior is simulated with a first-order transfer function with time constant T_G. The turbine transfer function includes the reheater time constant T_{RH}, the power fraction of the high pressure section of the turbine F_{HP}, and the time constant of the main inlet volume T_{CH}. R is the governor droop. The output of the turbine is the mechanical power variation ΔP_m. The equilibrium of the system is reached when the mechanical power is exactly equal to the electrical power. When the two powers are not balanced, the frequency deviation $\Delta\omega_r$ becomes non-zero. The system has inertia M and a load damping factor D, to emulate the load self-regulation [31]. The equivalent system parameters are listed in Table II. Several turbines with different time constants and transient behavior can be considered, however, the frequency support impact will not differ substantially from case to case. This power system linear model has been chosen due to the simplicity in analyzing mathematically the impact of the ST RTFR controller on the main grid, and in the implementation in the real time digital simulator for the PHIL evaluation.

In Fig. 5, the contribution of the STs is highlighted in blue. This system is a proof of concept and it is not meant as a real system application. The STs integrated in the distribution grid contribute to system frequency regulation with load power modulation ΔP_{ST}, defined by the droop curve of Fig. 4 and approximated in this analysis by means of linearization (neglecting the deadband effect) using a simple constant gain K_{dr}. The same gain of the droop characteristic is used for the linearization, with the effect that the following analysis is valid for when the system is outside the deadband area. The effect of the deadband on the frequency variation damping is negligible, as it will be shown in the experimental verification. The power variation contribution of each single ST is linked directly to the frequency change (Fig. 4, dashed line), and is defined by the relation

$$\Delta P_i = -K_{dr}\frac{f - f_0}{f_0} = -K_{dr}\Delta\omega \tag{4}$$

where, f and f_0 are the measured and nominal system frequency respectively, $\Delta\omega$ is the per unit frequency variation and ΔP_i is per unit power variation referred to nominal consumption of load L_i connected to ST$_i$. Assuming that all STs have the same droop, the total power modulation provided in response to frequency variation in per unit on total system load L_o is:

$$\Delta P_{ST} = -\frac{\sum L_i}{L_0}K_{dr}\Delta\omega = -K_{ST}K_{dr}\Delta\omega \tag{5}$$

where:

$$K_{ST} = \frac{\sum L_i}{L_0} \tag{6}$$

As seen above, K_{ST} indicates the amount of the power system load fed by STs, and it varies between 0 and 1. The remaining load $(1 - K_{ST})L_0$ remains synchronously connected, thus

it will respond to frequency variations $\Delta\omega$ with the self-regulation constant D. Referred to the total load L_0, this contribution is $D(1-K_{ST})$, as seen in Fig.5.

To analyze the RTFR controller contribution, the inner loop in Fig.5 is analyzed, without the effect of the conventional generation. The close-loop transfer function is defined as:

$$E(s) = \frac{1}{Ms + D(1-K_{ST}) + K_{ST}K_{dr}} = \frac{1}{Ms + D_{eq}} \quad (7)$$

where

$$D_{eq} = D + K_{ST}\left(K_{dr} - D\right) \quad (8)$$

As seen in (7), the ST RTFR controller effectively adds damping to the system. Note that K_{dr} is larger than D, for instance in Fig.4, K_{dr} is 5 pu, whereas self-regulation D is close to 1 pu.

To evaluate the effect of the ST-based RTFR control on the complete control system response, the close loop transfer function of the linear power system shown in Fig.5 is analyzed. The contribution to the equivalent conventional generator is:

$$E_{Gen}(s) = -\frac{1}{R}\frac{1}{1+sT_G}\frac{1+sF_{HP}T_{RH}}{(1+sT_{CH})(1+sT_{RH})} \quad (9)$$

The total contribution of generator and ST is then:

$$E_{Gen,ST}(s) = -K_{ST}K_{dr} + E_{Gen}(s) \quad (10)$$

and considering the system inertia M and load damping D transfer function:

$$I(s) = \frac{1}{Ms + D\left(1-K_{ST}\right)} \quad (11)$$

the response of the system frequency following an electrical load variation is described by the transfer function and the root locus shown in Fig.6:

$$\frac{\Delta\omega}{\Delta P_e} = \frac{I(s)}{1 + I(s)E_{Gen,ST}(s)} \quad (12)$$

In Fig.6a, the ST-controlled load share K_{ST} is increased from 0 % to 50 % (K_{ST}=0.5) in steps of 10%, considering a load damping equal to D=1. In all the aforementioned scenarios, a maximum controllable active power of 10 % has been assumed for each ST. Thus, the maximum load variation is 5 % of total system load for the highest considered ST penetration. The equivalent damping of the system increases from D_{eq}=1, in the case without RTFR control to D_{eq}=3.0 in case of 50 % ST-controlled load. The participation of the RTFR controller reduces the frequency oscillations, moving the poles toward the real axis of the root locus In a scenario of ST-controlled load of 20 %, the influence of the variable load damping (D varying within $[0-2]$ pu) is described in Fig.6b. As can be seen, the equivalent damping D_{eq} varies in the range 1-2.8 due to the contribution of RTFR controller. The comparison of the increase of the system inertia M and governor gain $1/R$ are shown in Fig.6c,d, respectively. It can be concluded that the RTFR controller enhances system capacity to handle frequency disturbances, avoiding the need to increase generator support, that may involve new investments.

TABLE I
EQUIVALENT SYSTEM PARAMETERS

Parameter	Value	Parameter	Value
R	0.05	T_G	0.2 s
T_{CH}	0.2 s	F_{HP}	0.3
T_{RH}	7 s	M	10 s
D	1	Kdr	5

The step response of the system is depicted in Fig.7a. Under a variation of 20 % of electrical load, the system frequency goes below 48.9 Hz. With the implementation of STs in the grid, the frequency variation decreases, and frequency stays above 49.2 Hz in case of 50 % ST-fed grid share. The response of the equivalent generator changes also in the presence of ST control. The RTFR algorithm supports the generator during the transient, reducing and damping the generator power response (Fig.7b). As a consequence of ST-based RTFR control, less generator regulation capability is needed in order to suppress large frequency variations. This represents an important feature for the power grids, mostly in those systems where building new generators or upgrading the old ones represent a challenge.

In the previous simulation results, a system inertia M=10 s was assumed. However, with the increasing integration of power electronics-based generators the inertia can decrease considerably. The cases with different system inertia are shown in Fig.8. The inertia is varied from 4 s to 12 s and the step response of the system has been evaluated. Two cases are simulated: (a) no ST control in the grid (Fig.8a); and (b) ST-fed load equal to 20 % of the total load and RTFR control active (Fig.8b). Two effects are noticeable: the RTFR control

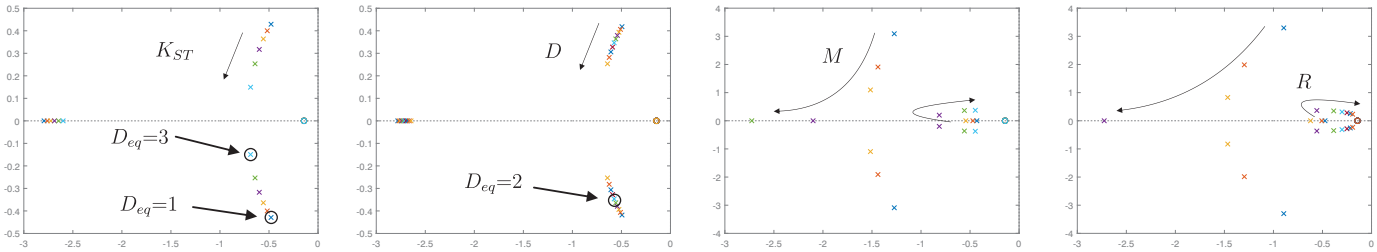

Fig. 6. Root locus of Eq.12 varying: (a) the ST-controllable load share K_{ST}, (b) the load damping D, (c) the generation inertia M, and (d) the generators droop characteristic $1/R$.

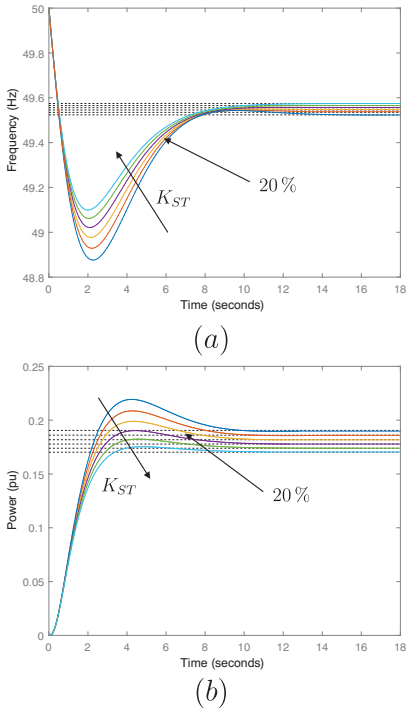

Fig. 7. System step response for increasing ST penetration K_{ST}: (a) Frequency variation in Hz; (b) Synchronous Generator response in per unit.

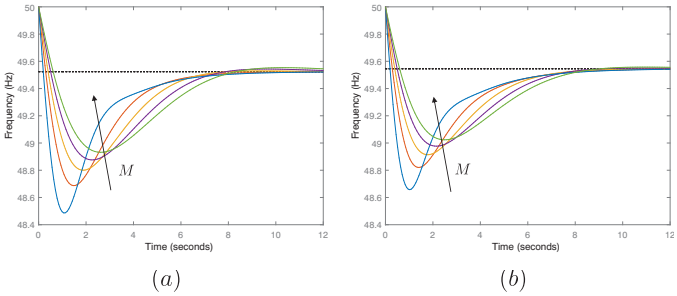

Fig. 8. Frequency variation with varying system inertia M: (a) no ST contribution; (b) ST contributes to 20 % of the total power.

reduces the negative frequency variation for all inertia values, and the system is better damped (this is more evident if the inertia is low, as for the case M=4 shown with light blue lines in the figures). Thus, the ST control can also partially compensate for synchronous generation inertia decrease.

IV. Power Hardware In Loop Evaluation

The effectiveness of the real time frequency support controller has been proved by means of PHIL evaluation, which scheme is shown in Fig. 9. The PHIL allows analyzing the behavior of the hardware under test (HuT), i.e. the ST, when connected to a large LV grid, not replicable in lab. In this specific case, the PHIL is used to investigate the performances of the RTFR controller implemented in the ST in real time conditions using real measurements from the ST-fed grid. The Hardware under Test, in this case the ST, controls the voltage v_L on the filter capacitor. The measurement system measures

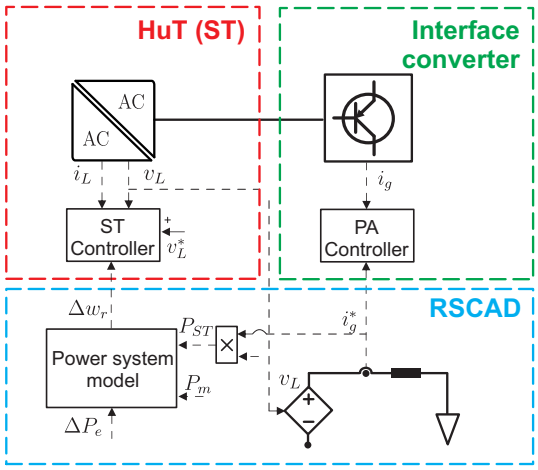

Fig. 9. PHIL: Hardware under Test (HuT) (red frame), Hardware of the PHIL setup (green frame), Software of the PHIL setup (RSCAD) (blue frame).

the voltage and sends the measurement signals v_L to the RTDS software, RSCAD. Here the voltage is applied directly in the ST-fed grid by means of an ideal controlled voltage source. The current demanded by the grid i_g^* is sampled in RTDS and sent to a current controller, that controls the current injection i_g of the linear power amplifier in order to reproduce accurately the grid current i_g^*, closing the loop. Between the simulated grid and the ST hardware, a current scale factor of 100 pu has been introduced in the current to cope with the limited power capability of the hardware in lab. It means that 1 kW power change in the hardware side corresponds to 100 kW power change in RSCAD at nominal voltage. The PHIL dynamic model has been presented in [32] [33], together with its stability and accuracy analysis.

To simulate the transmission grid, a power system equivalent model is realized in RSCAD. This model emulates the grid transient behavior during disturbances. The ST power measurement P_{ST} comes from the LV grid simulated in RSCAD and the machines mechanical power P_m and electrical power variation ΔP_e are external set point. The output of the power system model is the frequency deviation that is sent to the ST real time frequency support controller. The parameters of the ST setup are specified in Table II.

TABLE II
Experimental Setup Parameters.

Parameter	Value	Parameter	Value
$V_{dcL}(ST)$	700 V	$V_{dcL}(DG)$	700 V
S	4 kVA	L_L	5.03 mH
C_L	1.5 μF	v_L	230 V_{rms}
f_s	10 kHz	R_{dL}	2 Ω
Kp_v	0.1	Kr_v	200
Kp_i	0.75		

This work applies a modified version of the CIGRE European LV distribution network benchmark described in Chapter 3 and depicted in Fig. 10. The LV grid has been implemented in RSCAD and simulated with a time step of 45 μs, in the

range of the typical time steps used for PHIL applications [34].

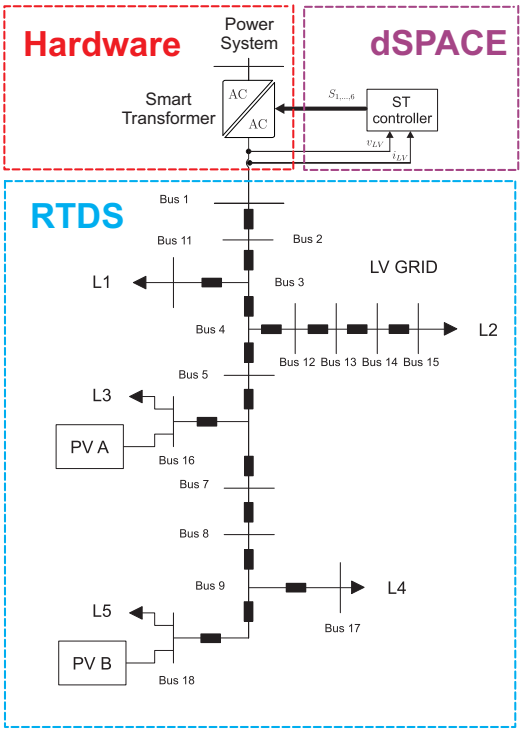

Fig. 10. modified CIGRE European LV distribution network benchmark implemented in RSCAD.

The CIGRE grid has been realized under the following assumptions: 1) the three-phase loads have been considered as constant current model and balanced, and 2) the photovoltaic power plants A and B are both injecting 20 kW, with power factor $cos(\phi)$=1. Table III itemizes the load power consumption and the position in the grid, while Table IV itemizes the location and power injection of the two PV power plants.

TABLE III
LOAD DATA

Load	Bus	Active Power (kW)	Reactive Power (kVAr)
L_1	11	25	10
L_2	15	50	30
L_3	16	45	20
L_4	17	5	5
L_5	18	20	5

TABLE IV
PV DATA

DER	Bus	Active Power (kW)	cosφ
PV A	16	20	1.00
PV B	18	20	1.00

V. EXPERIMENTAL RESULTS

The PHIL evaluation has been performed applying a electrical power variation ΔP_e to the equivalent power system in order to create under-frequency or over-frequency condition. In this Section the exact nonlinear power/frequency characteristic of Fig. 4 is implemented for the ST frequency control. Two events are considered in the PHIL evaluation: an under-frequency case, creates by an increase of the system load power request of 20 %; and an over-frequency case, caused by a decrease of the system load power equal to 20 %.

A. Under-frequency event

To simulate an under-frequency event, the power system electrical power P_e has been increased with a step of 20 %. This contingency can be the consequence of the loss of a big power plant or the disconnection of an area supplying the transmission system under investigation. From Fig. 11 plotted in RSCAD, it can be seen that without any control the frequency tends to decrease below 49 Hz.

Increasing the presence of ST in the grid (K_{ST}), two important effects can be noticed. Firstly, the transient frequency drop is reduced for increased ST participation. With 20 % ST presence in the grid, the frequency drop is reduced by 100 mHz, while for the case of half load controlled by ST (50 % case), the frequency drop is reduced by more than 200 mHz.

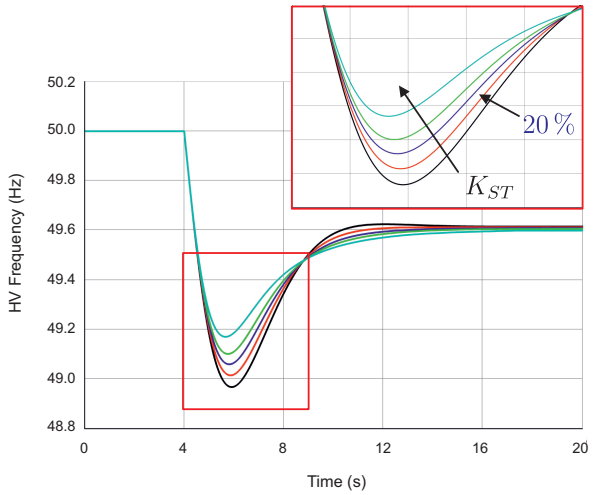

Fig. 11. System frequency during under-frequency condition

Secondly, the ST power deviation (ΔP_{ST}, Fig. 12) shows a faster control action than the conventional power system (governor and turbine). In Fig. 12, it can be noted how the ST presence helps to reduce the mechanical power transient peak ΔP_m, from 23 % to 20.5 % in case of 20 % ST-fed load, till it reaches an over-damped behavior in case of 50 % of ST-controlled load. Two major effects are achieved: the system power oscillations are more damped than the case without any control; the STs reduces the generator effort to reestablish a constant frequency value.

To depict the operation of the real time frequency controller in LV grid, the test case of 20 % ST-fed controlled load has been chosen. Applying the on-line load sensitivity identification, the grid K_P has been found equal to 1.25 pu. During the power variation in the power grid, and the following under-frequency conditions, the ST reduces the voltage set-point in

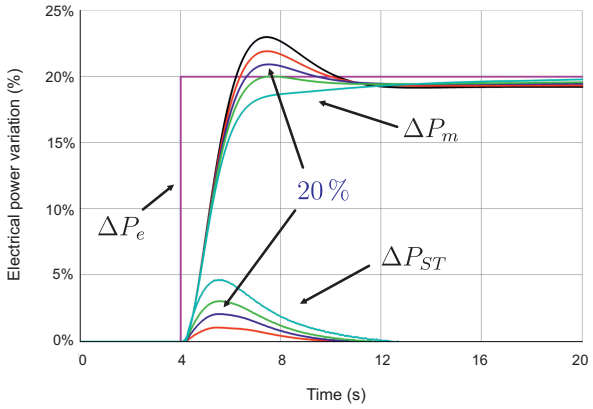

Fig. 12. System power during under-frequency condition

the grid up to 0.92 pu (Fig. 13). The grid experiences an under-voltage condition, with the buses farther from the ST slightly below 0.9 pu. However, this condition is found still acceptable due to the short duration of the under-voltage. The control, after a 20 second transient, restores the voltage nominal value in order to not affect the LV grid power quality.

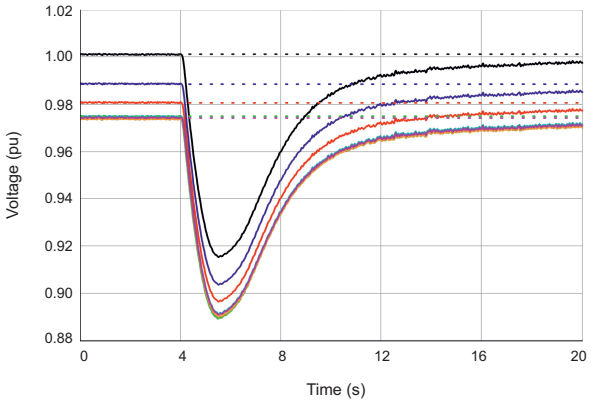

Fig. 13. Voltage profile in the LV grid during the RTFR controller operations (continuous lines) and without the RTFR controller operations (dashed lines), (20 % ST-fed controlled load).

In Fig. 14 the ST measured powers have been plotted. The first graph shows the measured active power in the hardware side. In the second graph the LV grid active (black line) and reactive (red line) power have been plotted. As can be noticed, there is a factor 100 between the measured power in hardware and software side. During the frequency transient, the frequency reaches almost 49 Hz. Following the droop characteristic in Fig. 4, it corresponds to a power variation of 10 %. The ST converter in the hardware side, varies the active power from 1.05 kW to 0.95 kW during the frequency negative peak, as expected from the droop characteristic. Where, the LV grid power consumption varies from 105 kW to 95 kW. This demonstrate the accuracy of the on-line load sensitivity identification algorithm.

B. Over-frequency event

Similarly to the under-frequency case, the ST is able to support the transmission grid during over-frequency transients.

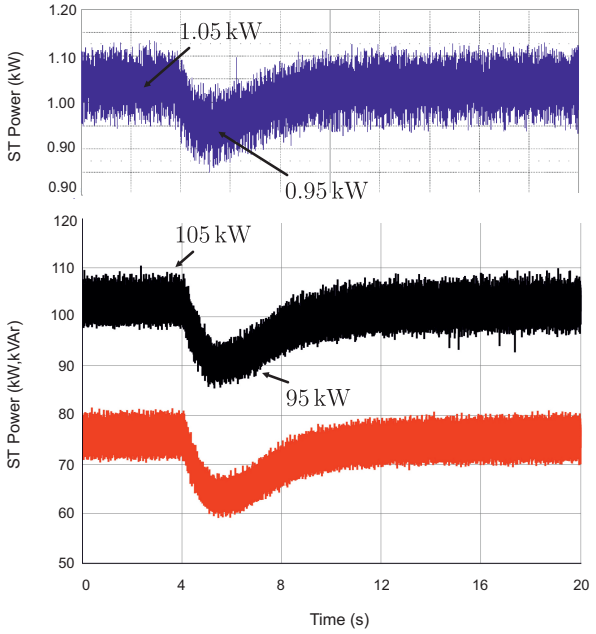

Fig. 14. ST (HuT) active power (blue line), ST (RSCAD) active (black line) and reactive (red line) power, (20 % ST-fed controlled load).

As can be noted in Fig. 15, the real time frequency controller of ST is able to reduce of 100 mHz or 200 mHz the frequency deviation in the 20 % and 50 % controlled load case, respectively. In terms of active power contribution (ΔP_{ST}), the ST contribution is similar to under-frequency case (Fig. 16). Increasing the presence of ST, the power contribution from the transmission grid generators ΔP_m is more damped.

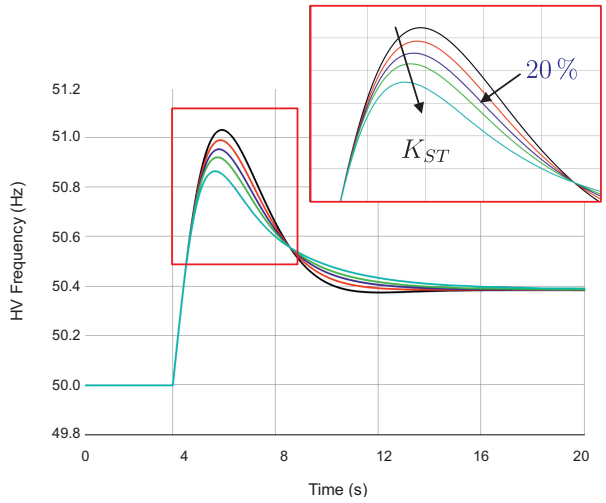

Fig. 15. System frequency during over-frequency condition

A substantial difference with respect to the under-frequency case can be noticed in the profile of the LV-grid voltage Fig. 17. The maximum voltage deviation in the grid is limited to +7 % and it is related to ST bus, while in the under-frequency case (Fig. 13), the voltage deviation reaches −11 % in the farther bus in the grid. The reason is the natural voltage drop in the LV grid, due to load absorption. For this reason, the maximum voltage variation in the ST-fed LV

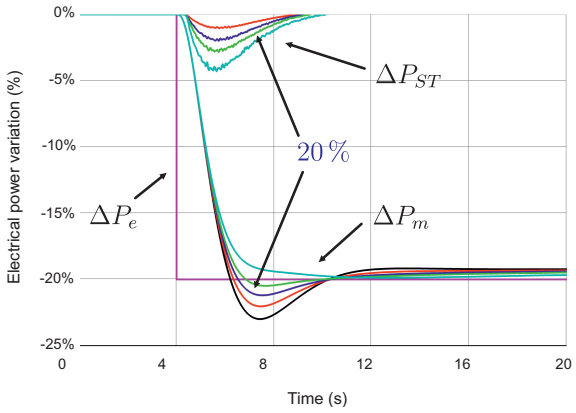

Fig. 16. System power during over-frequency condition

grid is higher in the under-frequency case than in the over-frequency one. The power availability of single ST depends also on the grid composition and power injection of the DG. In case of limited DG power injection, the real time frequency controller has more capability upwards (over-frequency case) than downwards (under-frequency case), and vice-versa in case of high DG power production.

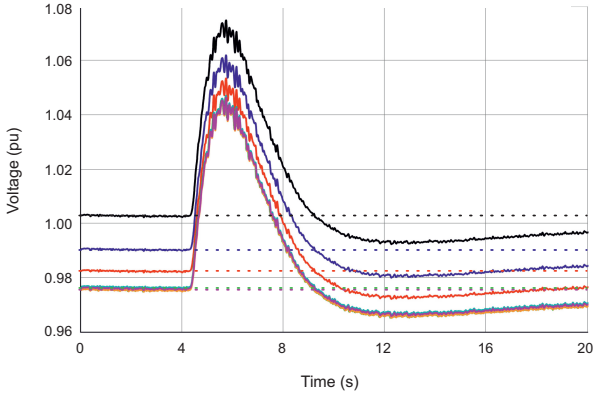

Fig. 17. Voltage profile in the LV grid during the frequency controller operations (continuous lines) and without the RTFR controller operations (dashed lines), (20 % ST-fed controlled load).

VI. Conclusion

In this paper, Smart Transformers are used to control the load consumption to provide primary frequency regulation to the transmission grid. By identifying the load sensitivity to voltage variations, the power can be accurately changed during a frequency transient to increase the equivalent system primary frequency regulation. In this work, it is proved that a 20 % of ST-controlled load is sufficient to decrease the transient frequency drop by 100 mHz in the power grid, avoiding to hit the load shedding schemes threshold (set to 49 Hz). Applying the ST-based RTFR control is equivalent to increase the load damping contribution, avoiding to request additional regulation capability from generators. The proposed frequency regulation service respects power quality limits (e.g. voltage variation in the ± 10 % range), but it may require some remuneration to the ST-fed loads (e.g., reduced bills).

References

[1] *"Contribution to Bulk System Control and Stability by Distributed Energy Resources connected at Distribution Network"*, IEEE PES Technical Report Std. TR22, 2017.

[2] B. Kroposki, B. Johnson, Y. Zhang, V. Gevorgian, P. Denholm, B. M. Hodge, and B. Hannegan, "Achieving a 100% renewable grid: Operating electric power systems with extremely high levels of variable renewable energy," *IEEE Power and Energy Magazine*, vol. 15, no. 2, pp. 61–73, March 2017.

[3] H. You, V. Vittal, and Z. Yang, "Self-healing in power systems: an approach using islanding and rate of frequency decline-based load shedding," *IEEE Transactions on Power Systems*, vol. 18, no. 1, pp. 174–181, Feb 2003.

[4] I. D. Margaris, S. A. Papathanassiou, N. D. Hatziargyriou, A. D. Hansen, and P. Sorensen, "Frequency control in autonomous power systems with high wind power penetration," *IEEE Transactions on Sustainable Energy*, vol. 3, no. 2, pp. 189–199, April 2012.

[5] G. Ramtharan, J. B. Ekanayake, and N. Jenkins, "Frequency support from doubly fed induction generator wind turbines," *IET Renewable Power Generation*, vol. 1, no. 1, pp. 3–9, March 2007.

[6] S. Pulendran and J. E. Tate, "Energy storage system control for prevention of transient under-frequency load shedding," *IEEE Transactions on Smart Grid*, vol. PP, no. 99, pp. 1–10, 2015.

[7] A. Oudalov, D. Chartouni, and C. Ohler, "Optimizing a battery energy storage system for primary frequency control," *IEEE Transactions on Power Systems*, vol. 22, no. 3, pp. 1259–1266, Aug 2007.

[8] C. Choniratisai, W. Pimjaipong, and L. Surapongpan, "Hvdc stability functions and implementation in thailand," in *15th Conference on Electric Power Supply Industry (CEPSI 2004)*, 2004.

[9] D. S. Callaway and I. A. Hiskens, "Achieving controllability of electric loads," *Proceedings of the IEEE*, vol. 99, no. 1, pp. 184–199, Jan 2011.

[10] J. A. Short, D. G. Infield, and L. L. Freris, "Stabilization of grid frequency through dynamic demand control," *IEEE Transactions on Power Systems*, vol. 22, no. 3, pp. 1284–1293, Aug 2007.

[11] Trudnowski, Donnelly, and Lightner, "Power-system frequency and stability control using decentralized intelligent loads," in *2005/2006 IEEE/PES Transmission and Distribution Conference and Exhibition*, May 2006, pp. 1453–1459.

[12] N. Lu and Hammerstrom, "Design considerations for frequency responsive grid friendly lt;sup gt;tm lt;/sup gt; appliances," in *2005/2006 IEEE/PES Transmission and Distribution Conference and Exhibition*, May 2006, pp. 647–652.

[13] A. Molina-Garcia, F. Bouffard, and D. S. Kirschen, "Decentralized demand-side contribution to primary frequency control," *IEEE Transactions on Power Systems*, vol. 26, no. 1, pp. 411–419, Feb 2011.

[14] E. McKenna, I. Richardson, and M. Thomson, "Smart meter data: Balancing consumer privacy concerns with legitimate applications," *Energy Policy*, vol. 41, pp. 807 – 814, 2012, modeling Transport (Energy) Demand and Policies. [Online]. Available: http://www.sciencedirect.com/science/article/pii/S0301421511009438

[15] A. Ballanti, L. N. Ochoa, K. Bailey, and S. Cox, "Unlocking new sources of flexibility: Class: The world's largest voltage-led load-management project," *IEEE Power and Energy Magazine*, vol. 15, no. 3, pp. 52–63, May 2017.

[16] A. Ballanti and L. F. Ochoa, "Voltage-led load management in whole distribution networks," *IEEE Transactions on Power Systems*, vol. 33, no. 2, pp. 1544–1554, March 2018.

[17] S. Y. Hui, C. K. Lee, and F. F. Wu, "Electric springsa new smart grid technology," *IEEE Transactions on Smart Grid*, vol. 3, no. 3, pp. 1552–1561, Sept 2012.

[18] C. K. Lee, N. R. Chaudhuri, B. Chaudhuri, and S. Y. R. Hui, "Droop control of distributed electric springs for stabilizing future power grid," *IEEE Transactions on Smart Grid*, vol. 4, no. 3, pp. 1558–1566, Sept 2013.

[19] X. Luo, Z. Akhtar, C. K. Lee, B. Chaudhuri, S. Tan, and S. Y. R. Hui, "Distributed voltage control with electric springs: Comparison with statcom," *IEEE Transactions on Smart Grid*, vol. 6, no. 1, pp. 209–219, Jan 2015.

[20] S. Tan, C. K. Lee, and S. Y. Hui, "General steady-state analysis and control principle of electric springs with active and reactive power compensations," *IEEE Transactions on Power Electronics*, vol. 28, no. 8, pp. 3958–3969, Aug 2013.

[21] ENTSOE-WGAS, "Survey on ancillary sservice procurement, balancing market design 2015," Tech. Rep., 2016.

[22] B. Zhou, H. Rao, W. Wu, T. Wang, C. Hong, D. Huang, W. Yao, X. Su, and T. Mao, "Principle and application of asynchronous operation of china southern power grid," *IEEE Journal of Emerging and Selected Topics in Power Electronics*, pp. 1–1, 2018.

[23] X. She, A. Huang, and R. Burgos, "Review of solid-state transformer technologies and their application in power distribution systems," *IEEE Journal of Emerging and Selected Topics in Power Electronics*, vol. 1, no. 3, pp. 186–198, Sept 2013.

[24] M. Liserre, G. Buticchi, M. Andresen, G. D. Carne, L. F. Costa, and Z. X. Zou, "The smart transformer: Impact on the electric grid and technology challenges," *IEEE Industrial Electronics Magazine*, vol. 10, no. 2, pp. 46–58, Summer 2016.

[25] G. De Carne, G. Buticchi, M. Liserre, and C. Vournas, "Load control using sensitivity identification by means of smart transformer," *IEEE Transactions on Smart Grid*, vol. PP, no. 99, pp. 1–1, 2016.

[26] G. D. Carne, M. Liserre, and C. Vournas, "On-line load sensitivity identification in lv distribution grids," *IEEE Transactions on Power Systems*, vol. 32, no. 2, pp. 1570–1571, March 2017.

[27] [Online]. Available: https://www.spenergynetworks.co.uk/pages/lv_engine.aspx

[28] J. Undrill, "Primary frequency response and control of power system frequency," Energy Analysis and Environmental Impacts Division Lawrence Berkeley National Laboratory, Tech. Rep., 2018. [Online]. Available: https://www.ferc.gov/industries/electric/indus-act/reliability/frequency-control-requirements/primary-response.pdf

[29] A. Bokhari, A. Alkan, R. Dogan, M. Diaz-Aguil, F. de Len, D. Czarkowski, Z. Zabar, L. Birenbaum, A. Noel, and R. E. Uosef, "Experimental determination of the zip coefficients for modern residential, commercial, and industrial loads," *IEEE Transactions on Power Delivery*, vol. 29, no. 3, pp. 1372–1381, June 2014.

[30] L. M. Korunovic, D. P. Stojanovic, and J. V. Milanovic, "Identification of static load characteristics based on measurements in medium-voltage distribution network," *IET Generation, Transmission Distribution*, vol. 2, no. 2, pp. 227–234, March 2008.

[31] P. Kundur, *Power System Stability and Control*. Electric Power Research Institute, 1994.

[32] G. D. Carne, G. Buticchi, and M. Liserre, "Current-type power hardware in the loop (phil) evaluation for smart transformer application," in *2018 IEEE International Conference on Industrial Electronics for Sustainable Energy Systems (IESES)*, Jan 2018, pp. 529–533.

[33] G. D. Carne, "Analysis of smart transformer features for electric distribution," Ph.D. dissertation, Kiel University, 2018. [Online]. Available: https://macau.uni-kiel.de/receive/dissertation_diss_00022905

[34] W. Ren, M. Steurer, and T. Baldwin, "Improve the stability and the accuracy of power hardware-in-the-loop simulation by selecting appropriate interface algorithms," *IEEE Transactions on Industry Applications*, vol. 44, no. 4, pp. 1286–1294, July 2008.

Giovanni De Carne (S'14-M'17) received the bachelor and master degrees in Electrical Engineering from Bari Ploytechnic (Italy) in 2011 and 2013, respectively. Since 2013 he works at the Chair of Power Electronics at Kiel University, Germany, where he got his PhD in 2018 with the thesis "Analysis of ST features for electric distribution grid" within the ERC Grant project "Highly Reliable And Efficient smart Transformer (HEART)". He is currently working as a post-doctoral researcher in the Kopernikus Project "ENSURE" in the HVDC control and services provision for HVAC grids.

Giampaolo Buticchi (S'10-M'13-SM'17) received the Master degree in Electronic Engineering in 2009 and the Ph.D degree in Information Technologies in 2013 from the University of Parma, Italy. In 2012 he was visiting researcher at The University of Nottingham, UK. Between 2014 and 2017, he was a post-doctoral researcher and Von Humboldt Post-doctoral Fellow at the University of Kiel, Germany. He is now Associate Professor in Electrical Engineering at The University of Nottingham Ningbo China and the Head of Power Electronics of the Nottingham Electrification Center. His research focuses on power electronics for renewable energy systems, smart transformer fed micro-grids and dc grids for the More Electric Aircraft. He is author/co-author of more than 160 scientific papers and an Associate Editor of the IEEE Transactions on Industrial Electronics.

Marco Liserre (S'00-M'02-SM'07-F'13) received the MSc and PhD degree in Electrical Engineering from the Bari Polytechnic, respectively in 1998 and 2002. He has been Associate Professor at Bari Polytechnic and Professor at Aalborg University (Denmark). He is currently Full Professor and he holds the Chair of Power Electronics at Kiel University (Germany). He has published over 300 technical papers (more than 100 of them in international peer-reviewed journals) and a book. These works have received more than 20000 citations. Marco Liserre is listed in ISI Thomson report The worlds most influential scientific minds. He is member of IAS, PELS, PES and IES. He has been serving all these societies in different capacities and he has received several IEEE awards.

Constantine (Costas) Vournas (S'77-M'87-SM'95-F'05) received the Diploma of Electrical and Mechanical Engineering from the National Technical University of Athens (NTUA) in 1975, the M.Sc in Electrical Engineering from the University of Saskatchewan, Saskatoon, Canada in 1978, and the NTUA Doctor of Engineering degree in 1986. He is currently Professor in the Electrical Energy Systems Laboratory of the School of Electrical and Computer Engineering of NTUA. He has co-authored the book Voltage Stability of Electric Power Systems. His research interests are in the area of power system dynamics, stability and control and include voltage stability and security analysis, wind generator integration in power systems, novel control applications in the distribution and transmission grid, as well as the effect of deregulation on power system operation and control.